

Article

# Analysis of A Remote Rainstorm in the Yangtze River Delta Region Caused by Typhoon Mangkhut (2018)

Jiaqi Yu <sup>1,2</sup>, Si Gao <sup>3,4,\*</sup> , Ling Zhang <sup>1,\*</sup>, Xinyong Shen <sup>1,4</sup> and Luyan Guo <sup>2</sup>

<sup>1</sup> Key Laboratory of Meteorological Disaster, Ministry of Education, and Collaborative Innovation Center on Forecast and Evaluation of Meteorological Disaster, Nanjing University of Information Science and Technology, Nanjing 210044, China; yujiaqi118877@163.com (J.Y.); shenxy@nuist.edu.cn (X.S.)

<sup>2</sup> Tongliao Meteorological Bureau of Inner Mongolia, Tongliao 028001, China; guoluyan123qxj@163.com

<sup>3</sup> School of Atmospheric Sciences, and Guangdong Province Key Laboratory for Climate Change and Natural Disaster Studies, Sun Yat-sen University, Zhuhai 519082, China

<sup>4</sup> Southern Marine Science and Engineering Guangdong Laboratory (Zhuhai), Zhuhai 519082, China

\* Correspondence: gaosi5@mail.sysu.edu.cn (S.G.); lingzhang@nuist.edu.cn (L.Z.); Tel.: +86-756-3668569 (S.G.)

Received: 26 March 2020; Accepted: 9 May 2020; Published: 12 May 2020



**Abstract:** An extraordinary heavy rain event caused by Typhoon Mangkhut occurred in the Yangtze River Delta region on 16 September 2018, with the maximum of 24-h accumulated rainfall at a single station reaching 297 mm. However, numerical models and subjective forecast failed to predict this typhoon remote rainstorm accurately. In this study, multiple observational data, an analysis dataset, and a trajectory model are used to analyze the causes of this severe rainstorm. The results show that the circulation situation provides a favorable large-scale background condition for the generation of the rainstorm. The coupling of the upper-level westerly jet and the low-level southerly jet is beneficial to the development of strong convections. In the rainstorm area there is a positive vorticity center connected to the main body of the typhoon. The cooling and humidifying effect of dry-cold air saturates the formerly unsaturated wet air, leading to the increase of precipitation. Besides, there is a lower-tropospheric moisture transport path connecting the typhoon and the rainstorm area, providing abundant moisture for the development of rainstorms. The backward trajectory simulation shows that the moisture mainly originates from the lower troposphere over the Philippine Sea, the southern South China Sea, and the sea south of the Philippines.

**Keywords:** typhoon remote rainstorm; Yangtze River Delta; moisture transport; upper and low-level jets

## 1. Introduction

Typhoons are one of the major disastrous weather systems causing extraordinary heavy rainfall in China. The typhoon-induced rainstorm areas can be roughly divided into the typhoon remote rainstorm (TRR) area and the rainfall area within the typhoon circulation (including rainstorm at the eye wall, precipitation inside and outside the spiral rain band, rainstorm in the inverted trough, rainstorm caused by the internal shear and rain in the squall line of the typhoon).

Several criteria have been proposed to identify the TRRs. Chen et al. [1] proposed that the typhoon remote precipitation should meet two requirements: first, the precipitation occurs outside the typhoon; second, there should be an internal physical connection of the precipitation with the typhoon. Cote [2] gave a statistical standard for typhoon remote rainstorm: first, the radar reflectivity factor exceeds 35 dBZ in the precipitation area, and the precipitation lasts for more than 6 h; second, the 24-h precipitation is  $\geq 100$  mm; third, there is a clear boundary between the remote rainfall area and the precipitation area within the typhoon circulation in radar images, and moreover, there is a moisture transport path connecting the typhoon and the TRR area.

Previous studies have pointed out that the interaction between the typhoon and mid-latitude systems (low trough cold front, Northeast Cold Vortex, Southwest Vortex, upper and low-level jets, weak cold air, etc.) can lead to more significant precipitation in mid-latitude inland areas, namely the TRR [3,4]. After studying 28 TRRs to the east of the Rocky Mountains in the United States from 1995 to 2008, Galarna and Bosart [5] found that TRRs are more likely to occur in the regions to the east of the upper trough at 700 hPa, the west of the ridge line in the potential temperature field at 925 hPa, and at the entrance of the upper level jet at 200 hPa. Byun and Lee [6] analyzed TRR events on the Korean Peninsula from 1981 to 2009 and concluded that the average annual rainfall of remote rainstorms caused by tropical cyclones during this period accounts for 49% of the 29-year-average total annual rainfall. Moreover, the circulation situation during these remote rainstorm events shows that tropical cyclones are generally located over the southwestern Korean Peninsula, with a trough to its northwest, and the western Pacific subtropical high lies to the southeast of tropical cyclones. Sensitivity experiments revealed that Typhoon Songda (2004) in the south of the Northwest Pacific Ocean was crucial to the heavy precipitation in central Japan and its adjacent sea areas [7]. Zhou et al. [8] analyzed all the typhoons landfalling north of Shantou, South China, from 1987 to 1992. The results showed that the onshore activities of landfalling typhoons and the characteristics of corresponding TRRs are related to the offshore activities of those typhoons. The formation of remote rainstorms caused by landfalling typhoons is related to the mesoscale warm sectors in the low-level southeasterly jets before and after the typhoon's landfall. Moreover, the locations of rainstorm are related to the relative positions of mesoscale warm sectors between the typhoon and subtropical high.

The TRR is hard to predict due to its low frequency of occurrence and the difficulties in establishing a synoptic conception model. However, the corresponding disasters due to TRRs generally exceeds that of rainstorms within the typhoon circulation. An extraordinary heavy rain event occurred in the Yangtze River Delta region on 16 September 2018, later we will show that it was a TRR caused by Typhoon Mangkhut (2018). Given that the TRRs in the Yangtze River Delta have not been paid much attention in previous studies, it is desirable to explore the causes of this TRR event in detail. In this study we adopt a comprehensive data collection, which consists of the U.S. National Centers for Environmental Prediction (NCEP) operational Global Forecast System (GFS) 6-hourly analysis data with the resolution of  $0.25^\circ$ , the observation data from surface automatic weather stations and sounding stations in China, the hourly precipitation data with the resolution of  $0.1^\circ$ , which is merged with the observation data in China and CMORPH (Climate Prediction Center Morphing technique) data. By combining with the Hybrid Single-Particle Lagrangian Integrated Trajectory (HYSPLIT) model, a diagnostic analysis will be conducted on the circulation situation, thermodynamic and dynamic conditions, and trigger mechanisms of the TRR. Through this case study, we aim for a better understanding of TRRs, especially in the Yangtze River Delta region.

## 2. Case Overview

### 2.1. Typhoon Mangkhut

At 1200 UTC 7 September 2018, Typhoon Mangkhut generated in the southeastern part of the Northwest Pacific and rapidly intensified to a super typhoon on the early morning of 11 September. At 1820 UTC 14 September, Mangkhut made landfall in the northern Luzon island of the Philippines as a super typhoon. After that, Mangkhut weakened to a severe typhoon and entered the South China Sea, while its huge circulation and vast cloud system still maintained. Data from both the China National Meteorological Center (NMC) and the Japan Meteorological Agency (JMA) showed that Mangkhut had the radius of gale-force wind over 500 km. At 0900 UTC 16 September, Mangkhut landed at Taishan, Guangdong Province of China (the locations mentioned here and hereafter are indicated in Figure 1), as a severe typhoon. On the afternoon of 16 September, it was extremely muggy in the Yangtze River Delta (i.e., Jiangsu Province, Zhejiang Province, and Shanghai), located far from the typhoon center, and cumulonimbus clouds took the lead to develop rapidly in Jiangsu Province.

Changshu was the first city struck by the torrential rain, and the rainfall amount within 24 h was close to 300 mm (Table 1), which exceeded the maximum 24-h precipitation in the Pearl River Delta where the main body of Mangkhut was located. Subsequently, torrential rain also occurred at some stations in Zhejiang Province and Shanghai. Afterwards, Mangkhut began to weaken and continued to move northwestward until its dissipation.

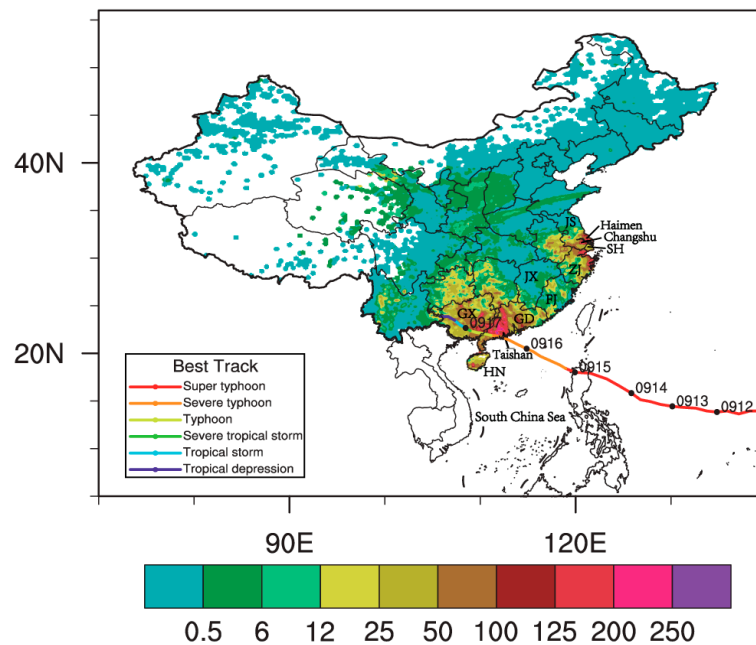


**Figure 1.** Observed 24-h precipitation amount (mm) during 0000 UTC 16 September to 0000 UTC 17 September 2018 and track of Typhoon Mangkhut after 11 September 2018. Locations of Guangdong (GD), Guangxi (GX), Hainan (HN), Fujian (FJ), Jiangxi (JX), Zhejiang (ZJ), Jiangsu (JS) Provinces and Shanghai (SH), Haimen, Changshu, and Taishan Cities are marked.

**Table 1.** Top 10 stations with the largest 24-h precipitation amount during 0000 UTC 16 September to 0000 UTC 17 September 2018.

Ranking	Station Number	Station Name	Province	Precipitation Amount (mm)
01	58352	Changshu	Jiangsu	296.7
02	59663	Yangjiang	Guangdong	254.8
03	58360	Haimen	Jiangsu	232.1
04	59493	Shenzhen	Guangdong	218.5
05	58470	Xinxing	Guangdong	210.7
06	59469	Yangchun	Guangdong	207.8
07	58455	Haining	Zhejiang	205.8
08	59298	Huizhou	Guangdong	201.4
09	59297	Boluo	Guangdong	198.6
10	58478	Taishan	Guangdong	197.8

### 2.2. Precipitation Observation

During 0000 UTC 16 September to 0000 UTC 17 September 2018, heavy rainfall occurred in the southern Jiangsu Province and northern Zhejiang Province (Figure 1), with the rain belt extending from east to west. The maximum of 24-h precipitation (297 mm) occurred at Changshu (Table 1), and the maximum hourly precipitation (93 mm, between 0300 and 0400 UTC 16 September) occurred at Haimen (Figure 2). After 1600 UTC 16 September, the precipitation intensity decreased significantly, indicating the abruptness and high efficiency of this precipitation event.

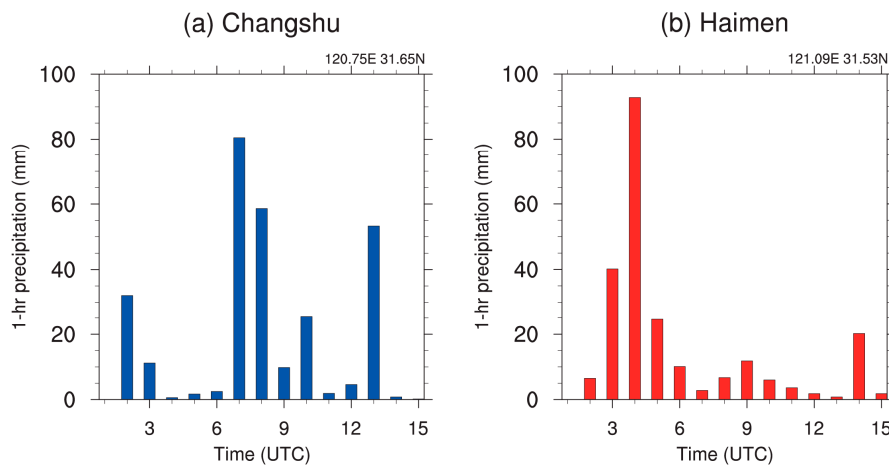


**Figure 2.** Time series of 1-h precipitation amount (mm) at (a) Changshu and (b) Haimen during 0100-1500 UTC 16 September 2018.

### 2.3. Identification of TRR

It is known that the rainfall would increase with the establishment of moisture transport paths [9]. Moisture flux at 850 hPa shows that a strong moisture transport path gradually broke away from the typhoon and moved northeastward at 0000 UTC 16 September before the rainstorm occurred (Figure 3a). At 0600 UTC 16 September, the exit of the moisture transport path moved to the Yangtze River Delta. Thus, a strong moisture transport path connecting the typhoon and the rainstorm area was established, transporting very moist, unstable airmass to the rainstorm area (Figure 3b). At 1800 UTC 16 September, the moisture transport path separated from the typhoon and weakened afterwards (Figure 3c,d), meanwhile, the rainfall intensity also gradually decreased.

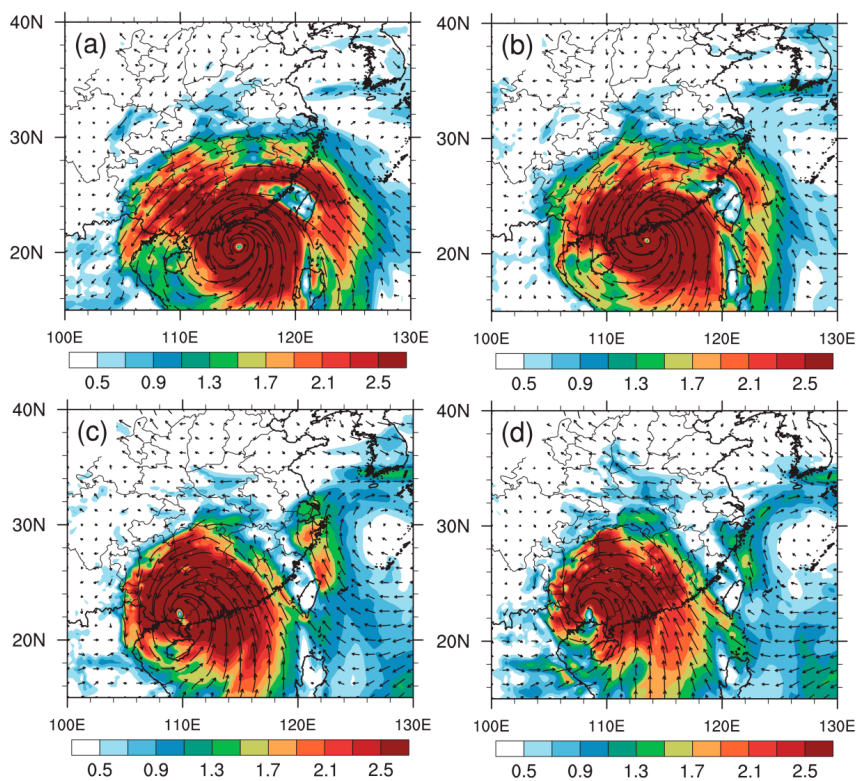


**Figure 3.** Moisture transport ( $10^{-1} \text{ g m}^{-1} \text{ s}^{-1} \text{ hPa}^{-1}$ ) at 850 hPa at (a) 0000 UTC 16 September, (b) 0600 UTC 16 September, (c) 1800 UTC 16 September, and (d) 0000 UTC 17 September 2018.

According to the distribution of the 24-h precipitation (Figure 1) and the corresponding radar echo images (figures omitted), there was a clear boundary, which lay in Fujian and Jiangxi Provinces (see their locations in Figure 1), between the remote precipitation area and the precipitation area within the typhoon circulation. The precipitation persisted for more than 6 h (Figure 2), and the radar reflectivity in the precipitation area was  $\geq 35$  dBZ (figures omitted). All these aspects indicate that the rainstorm was a TRR caused by Mangkhut in the Yangtze River Delta, according to the criteria given in [2].

#### 2.4. Precipitation Forecast

Among numerical predictions for the rainfall during 0000 UTC 16 September to 0000 UTC 17 September by several models, the TRR can only be predicted by the East China Model. The model is based on the Weather Research and Forecasting (WRF) v3.5.1 and uses NCEP GFS analysis as the first guess. It has 51 vertical levels with a horizontal resolution of 9 km and a domain size of  $760 \times 600$  which covers all of China [10]. However, the predicted range of the rainstorm was smaller and the predicted location shifted southwestward from the observation. None of other models, including the ECMWF (European Centre for Medium-Range Weather Forecasts) model, the NCEP GFS model, and the Japan Global Spectral Model (GSM), could predict the TRR event (figures omitted). The China NMC only predicted heavy rains in the south-central Jiangsu Province and southeastern Zhejiang Province, and downpours in parts of south-central Guangdong Province, southeastern Guangxi Province, and northeastern Hainan Province (figure omitted). Therefore, neither the numerical forecasts from various sources nor the subjective forecast from the China NMC could predict this torrential rain in the Yangtze River Delta. The causes of the rainstorm will be analyzed in detail in the following section.

### 3. Causes of the TRR

#### 3.1. Large-Scale Circulation Situation

At 500 hPa, East China had been dominated by the subtropical high since 13 September. The precipitation during 13-14 September brought humid air, thus leading to muggy weather in this region. Before the rainstorm, the subtropical high extending from east to west controlled South and East China, with a central intensity of 592 dagpm, and the line of 588 dagpm extended westward to around  $95^\circ\text{E}$ . The Mongolia cold vortex moved eastward and strengthened with the supplement of the cold air from higher latitudes, forming a wide trough area in Northeast and North China. The upper trough extending southward from the Mongolia cold vortex split into two parts, the north trough moved quickly with the cold vortex while the south trough moved slowly because of the obstruction of the subtropical high (Figure 4a). As Mangkhut landed in Guangdong and moved northwestward, the subtropical high retreated eastward to the middle and lower reaches of the Yangtze River and the south trough moved eastward to North China at 1200 UTC 16 September (Figure 4b). The southern Jiangsu Province was in the southwest air flow at the inner edge of the subtropical high until 1800 UTC 16 September (Figure 4c). Afterwards, Mangkhut gradually weakened.

At 850 hPa, Central China was under the control of continental high, and East China was in the middle of four systems: continental high, subtropical high, typhoon, and Mongolia cold vortex, leading to weak winds in the two regions at 1800 UTC 15 September. Meanwhile, the north trough was still located south of the cold vortex and the south trough disappeared due to the influence of continental high. A strong and narrow southerly low-level jet occurred east of the typhoon center (Figure 4d). At 0600 UTC 16 September, with the northwest movement of the typhoon, the warm shear to the northeast of the typhoon shifted northward to around  $30^\circ\text{N}$  (Figure 4e), and the rainstorm occurred in the Yangtze River Delta. At 1800 UTC 16 September, with a gradual weakening and westward movement of the typhoon, the continental high and the subtropical high intensified and the rainstorm area gradually narrowed (Figure 4f). This suggests that the northward shift of the warm shear is favorable for the establishment of the unstable stratification and the rapid generation and development of convective clouds.

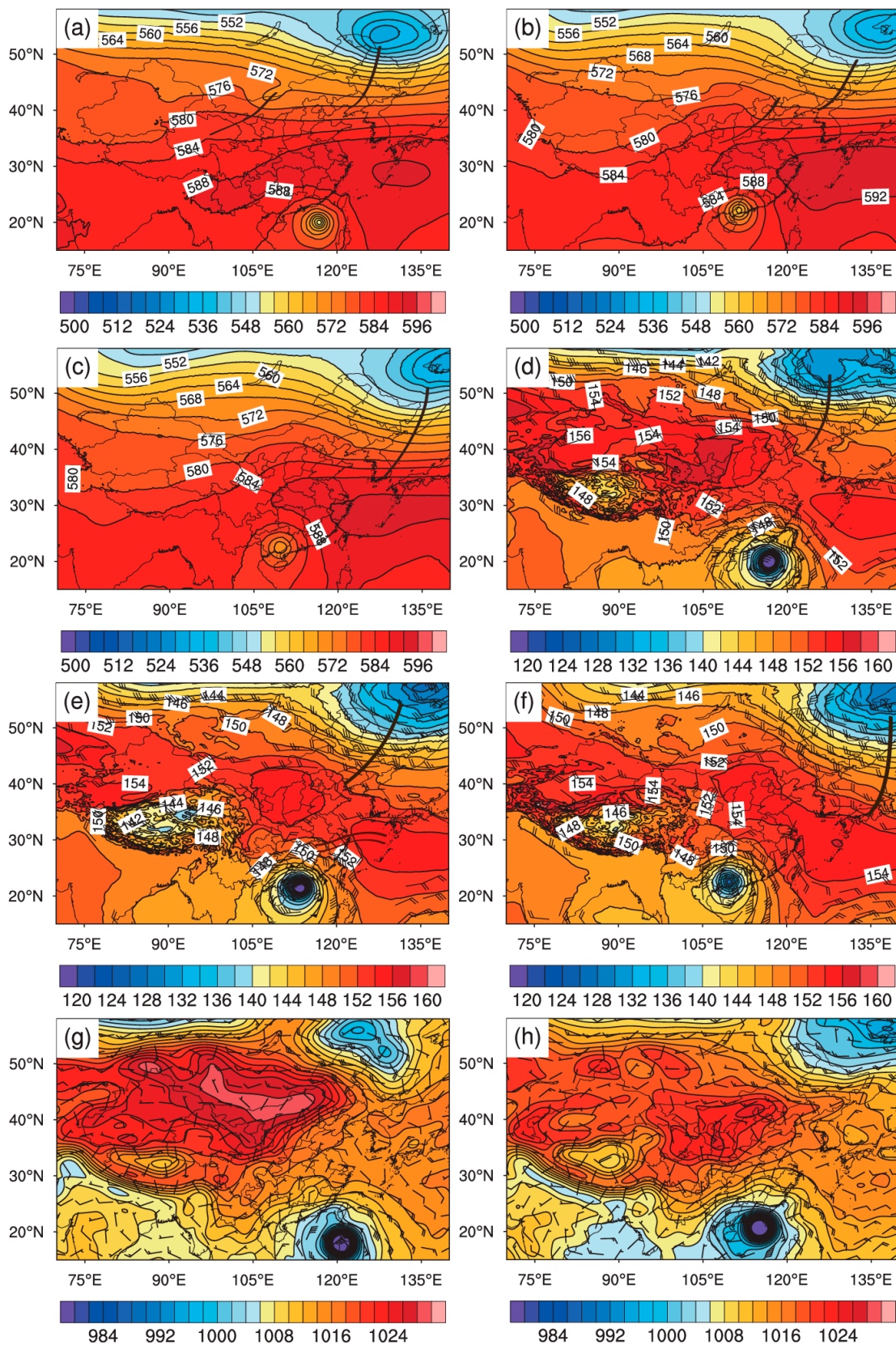


**Figure 4.** Geopotential height (dagpm) at 500 hPa at (a) 1800 UTC 15 September, (b) 1200 UTC 16 September, and (c) 1800 UTC 16 September 2018, geopotential height (dagpm) and winds ( $m \cdot s^{-1}$ ) at 850 hPa at (d) 1800 UTC 15 September, (e) 0600 UTC 16 September, and (f) 1800 UTC 16 September 2018, and sea level pressure (hPa) at and winds ( $m \cdot s^{-1}$ ) at (g) 0000 UTC 15 September and (h) 0000 UTC 16 September 2018. Thick curves denote troughs lines.

In the sea level pressure field, the continental high and the subtropical high firstly merged (Figure 4g), while the land surface temperature remained above 30 °C. During the northward movement of the typhoon, the two high-pressure systems gradually separated and the subtropical high retreated eastward. At that time, the southern Jiangsu Province was in the convergence zone between the two high-pressure centers (Figure 4h), leading to persistent high temperature and humidity in this region.

### 3.2. Upper and Low-Level Jets

At 0600 UTC 16 September, a westerly jet at 200 hPa was located in mid-latitudes, with a central intensity of 60 m·s<sup>-1</sup> (Figure 5a). The upper-level jet is favorable for the development and maintenance of convection in two ways. Firstly, the associated strong vertical wind shear under the jet can benefit the enhancement of mass divergence at the top of convective clouds and therefore the development and maintenance of updrafts. Secondly, the latent heat released by the condensation of water vapor during the development of convective clouds can warm the upper part of the clouds and tend to stabilize the atmospheric stratification, while the strong wind at upper levels can remove the warming air from the upper part of the clouds, leading to a ventilation effect, which is conducive to the maintenance and development of the convective clouds [11].

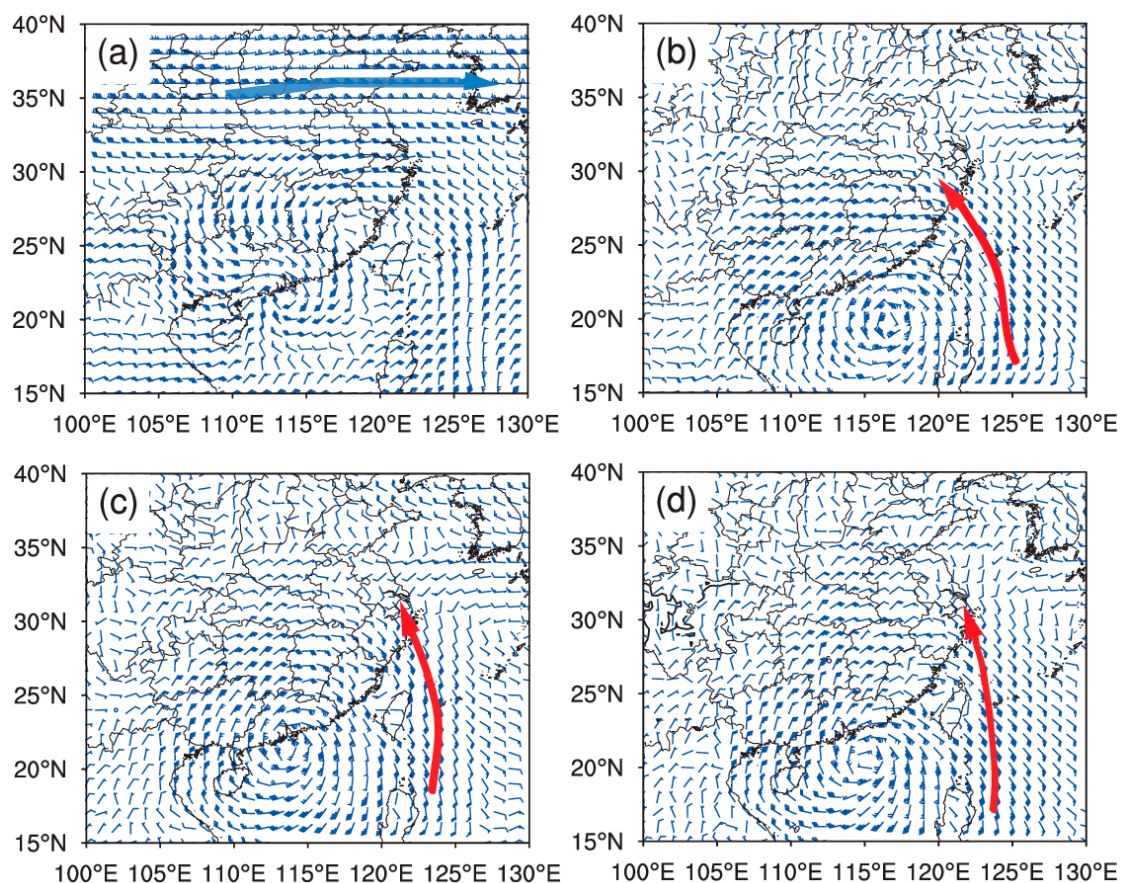


**Figure 5.** Winds (m·s<sup>-1</sup>) (a) at 200 hPa at 0600 UTC 16 September, at 850 hPa at (b) 1800 UTC 15 September and (c) 0600 UTC 16 September, and (d) at 925 hPa at 0000 UTC 16 September 2018. Blue arrow in (a) denotes the upper-level jet and red arrows in (b–d) denote the low-level jets.

At 850 hPa, a strong and narrow southerly jet gradually formed east of the typhoon at 1800 UTC 15 September (Figure 5b). The southerly jet was away from the typhoon and reached its peak intensity, with the exit region located around the Yangtze River Delta (Figure 5c). The southerly jet maintained

till 1800 UTC 16 September and then began to weaken. At 925 hPa, an ultra-low-level jet developed at 0000 UTC 16 September, with the central intensity reaching  $16 \text{ m}\cdot\text{s}^{-1}$  (Figure 5d). The rainstorm was in the positive shear vorticity area on the left of the exit region of the low-level jets. There were significant moisture and mass convergence in the front left of the jet streak, which led to strong upward motion. The low-level jet has strong thermodynamic and dynamic instability; it acts as a conveyor belt of heat and moisture for a rainstorm, and the associated wind velocity fluctuations can trigger mesoscale convective systems and rain clusters [12,13].

The adjustment of thermal wind in baroclinic atmosphere is conducive to the unstable development of northward-propagating inertial gravity waves. The strong baroclinity in the entrance region of an upper-level jet provides favorable conditions for the unstable inertial gravity waves. This instability can induce strong thermally direct circulation and result in strong ascending motion south of the entrance region of the upper-level jet [14,15]. The superposition of the ascending motion and a low-level jet in the south can strengthen the low-level jet, which is favorable for the generation of rainstorm and the northward advance of rain zone [16]. As a result, the coupling of the upper- and low-level jets was a cause for the occurrence of this TRR event and for the increase in rainfall.

### 3.3. Sounding Analysis

Dry air intrusion is generally accompanied with high potential vorticity, and the high potential vorticity area at 500 hPa corresponds well to the precipitation area [17]. Sounding maps can intuitively show the heights of dry air intrusions. Before the rainstorm, the high temperature and humidity in East China were favorable for the accumulation of instability. At 0000 UTC 16 September, the sounding at Baoshan Station of Shanghai (No. 58362) showed a dry-cold air intrusion near 500 hPa and an inversion layer near 850 hPa (Figure 6a). As Mangkhut moved northwestward and the southwesterly jet strengthened, the low-level air gradually became saturated. The dry-cold air intrusion continued till 0600 UTC 16 September. There were deep wet and unstable layers above the ground, which extended upward to 500 hPa. Meanwhile, the convective available potential energy was as high as  $3067 \text{ J}\cdot\text{Kg}^{-1}$  (figure omitted). Numerical simulation of a TRR affecting North China found that dry-cold air intrusion from the upper layer can increase convective instability in the precipitation area and saturate the formerly unsaturated humid air, leading to the increase in precipitation [18]. Thus, the increase in rainfall around 0600 UTC 16 September can be partially attributed to the dry-cold air intrusion. At 1200 UTC 16 September, the dry air intrusion disappeared (Figure 6b). Although there was still a large amount of instability, the precipitation intensity gradually weakened afterwards.

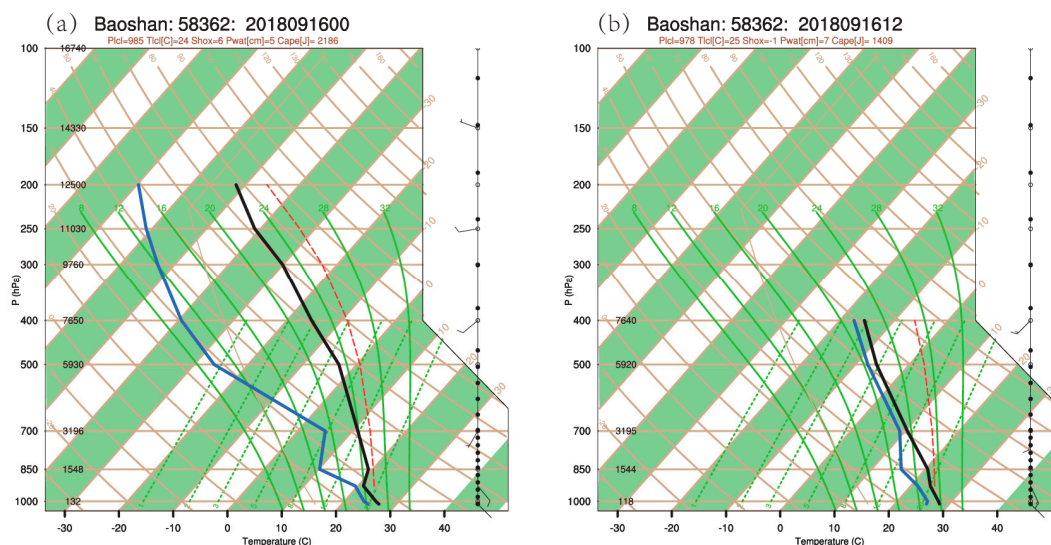
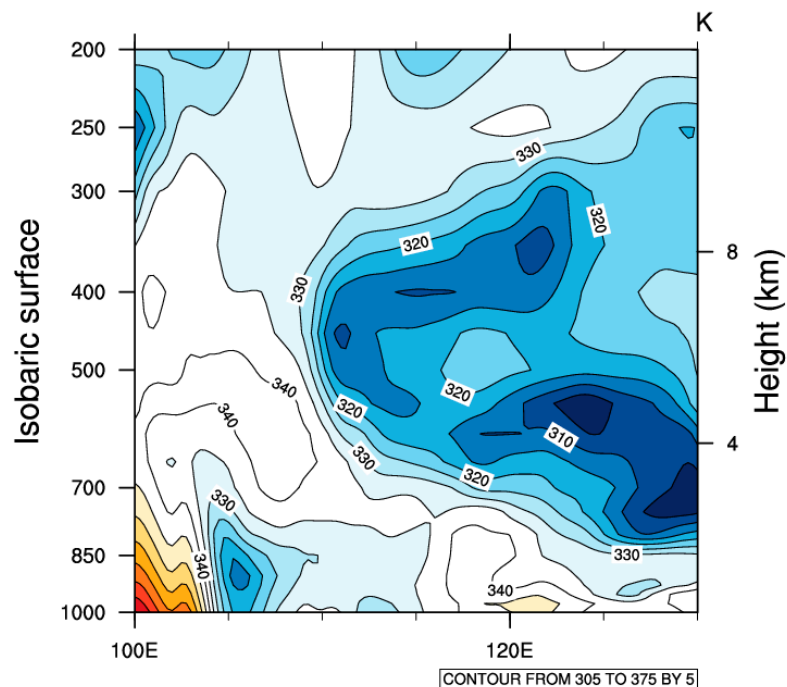


Figure 6. Soundings at Baoshan Station (No. 58362) in Shanghai at (a) 0000 UTC and (b) 1200 UTC 16 September 2018.

### 3.4. Thermodynamic Conditions

The spatial distribution of potential pseudo-equivalent temperature ( $\theta_{se}$ ) at 850 hPa at 0000 UTC 16 September (figure omitted) shows a high  $\theta_{se}$  area to the south of 30°N and a low  $\theta_{se}$  area was to the north of 38°N. Therefore, there was a dense gradient region of  $\theta_{se}$  in 30–38°N, presenting a roughly east–west orientation. The southern Jiangsu Province was at the front edge of the northward-extending high-energy tongue. After 0600 UTC 16 September, the dense gradient region of  $\theta_{se}$ , which presented a northeast–southwest orientation, shifted northward by about two degrees in latitude, with a slight strengthening and a marked eastward extension. At that time, the southern Jiangsu Province was still at the front edge of the high-energy tongue. The front edge of the northward-extending high-energy tongue was basically consistent with the heavy precipitation area. The longitude-vertical cross section of  $\theta_{se}$  along 32°N (Figure 7) indicates a convectively unstable stratification near 120°E where  $\theta_{se}$  decreased with height from 1000 to 600 hPa, a dry-cold air intrusion at 500 hPa, and a frontal zone at 700 hPa at 0000 UTC 16 September. All these conditions were favorable for the accumulation of energy for the occurrence of the TRR event.



**Figure 7.** Longitude-vertical cross section of pseudo equivalent potential temperature (K) along 32°N at 0000 UTC 16 September 2018.

### 3.5. Dynamic Conditions

The typhoon inverted trough at 850 hPa appeared as a cyclonic vorticity band at 0000 UTC 16 September (Figure 8a). However, due to the non-uniform wind shear in the inverted trough, a northwest–southeast oriented positive vorticity band with a strengthened center appeared at the northern end of the inverted trough. At 0600 UTC 16 September (Figure 8b), as the southeasterly low-level jet enhanced and moved northward, the cyclonic shear near the top of the inverted trough strengthened, and the corresponding vorticity center moved northward to the border area between Zhejiang and Fujian Provinces. Until 1200 UTC 16 September, the cyclonic vorticity centers at both the northern end of the inverted trough and the main body of Mangkhut weakened, and the two vorticity centers tended to separate (Figure 8c). At 0000 UTC 17 September, the cyclonic vorticity center at the northern end of the typhoon inverted trough completely separated from the typhoon circulation (Figure 8d). The longitude-vertical cross section of divergence (Figure 9a) shows strong convergence at 1000–925 hPa and strong divergence around 300 hPa during the rainstorm. The increase

in divergence at upper levels corresponded to the strengthening of upper-level jets. The vorticity field (Figure 9b) shows that the positive vorticity zone was below 850 hPa. Combining with the location of heavy precipitation center, it is indicated that the upward motion was not very strong during the precipitation, and the precipitation was mainly contributed by moisture and instability transported by the low-level jets. This further illustrates that the remote transportation of moisture and energy by Mangkhut played an important role in the formation of the torrential rain.

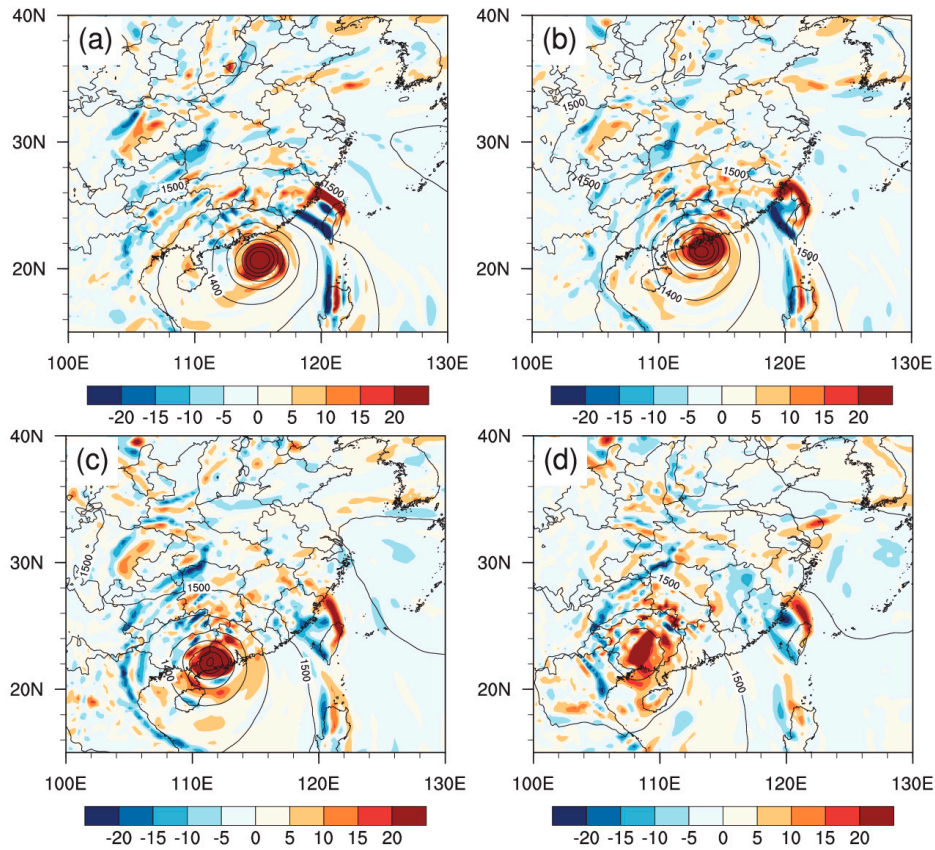


**Figure 8.** Relative vorticity ( $10^{-5} \text{ s}^{-1}$ ) at 850 hPa at (a) 0000 UTC 16 September, (b) 0600 UTC 16 September, (c) 1200 UTC 16 September, and (d) 0000 UTC 17 September 2018.

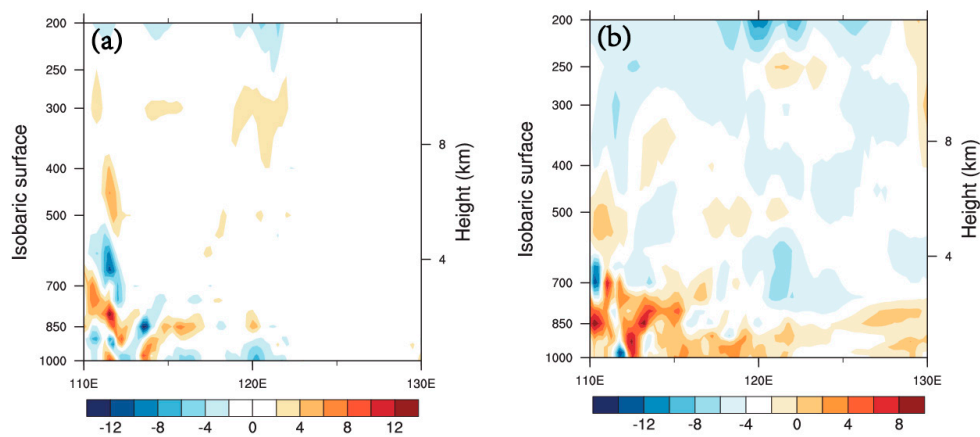


**Figure 9.** Longitude-vertical cross section of (a) divergence ( $10^{-5} \text{ s}^{-1}$ ) and (b) relative vorticity ( $10^{-5} \text{ s}^{-1}$ ) along  $32^\circ\text{N}$  at 0600 UTC 16 September 2018.

### 3.6. Simulation of Moisture Transport

The Euler method can be used to analyze the source and amount of moisture, but how the moisture reaches the precipitation area and how the moisture distributes at different stages and in different regions remain unsolved. These questions are further discussed below by using the air parcel tracing technique based on the Lagrangian method. The version 4 of HYSPLIT [19,20] developed by the U.S. National Oceanic and Atmospheric Administration (NOAA) was used to track the trajectory of multiple air parcels around (120°E, 30°N) above the ground for 120 h before 0600 UTC 16 September. According to the above analyses, the moisture transport paths over the TRR area were mainly below 850 hPa during the precipitation. The heights of 1000, 1500, and 2000 m were therefore chosen as the starting levels for backward trajectory simulations of air parcels, consistent with [21].

Figure 10 shows the simulated 120-h backward trajectories and the associated relative humidity of multiple air parcels at the three heights in the rainstorm area at 0600 UTC 16 September. There were obvious differences among trajectories before 0000 UTC 14 September. Air parcels at the three heights can originate from the sea south of the Philippines, the southern South China Sea, or the Philippine Sea. The trajectories of air parcels at the three heights were similar after 0000 UTC 14 September, mostly with a significant cyclonic curvature. As Mangkhut gradually moved from the northwestern Philippines to Taishan, South China during 14–16 September, air parcels at the three heights moved northwestward along the peripheral airflow of Mangkhut and finally reached the Yangtze River Delta. Regarding the evolution of heights, the moisture transport paths were generally below 1500 m since 0000 UTC 13 September, further indicating that the moisture source of the rainstorm was mainly from the layer below 850 hPa, corresponding to the positive vorticity zone and the strong convergence zone. From 1200 UTC 15 September to 0600 UTC 16 September, the low-level moist airmasses at the three heights were uplifted rapidly, corresponding to the generation of the rainstorm. Regarding the evolution of relative humidity, the air parcels at the path of 1000 m were always very moist. The air parcels at the paths of 1500 and 2000 m moistened obviously during 11–13 September. The results suggest that typhoon circulation played a crucial role in transporting moisture to the TRR area and that the moisture for this rainstorm was mainly from the Philippine Sea, the sea south of the Philippines, and the southern South China Sea. Physical mechanisms responsible for this TRR event are summarized in Figure 11.

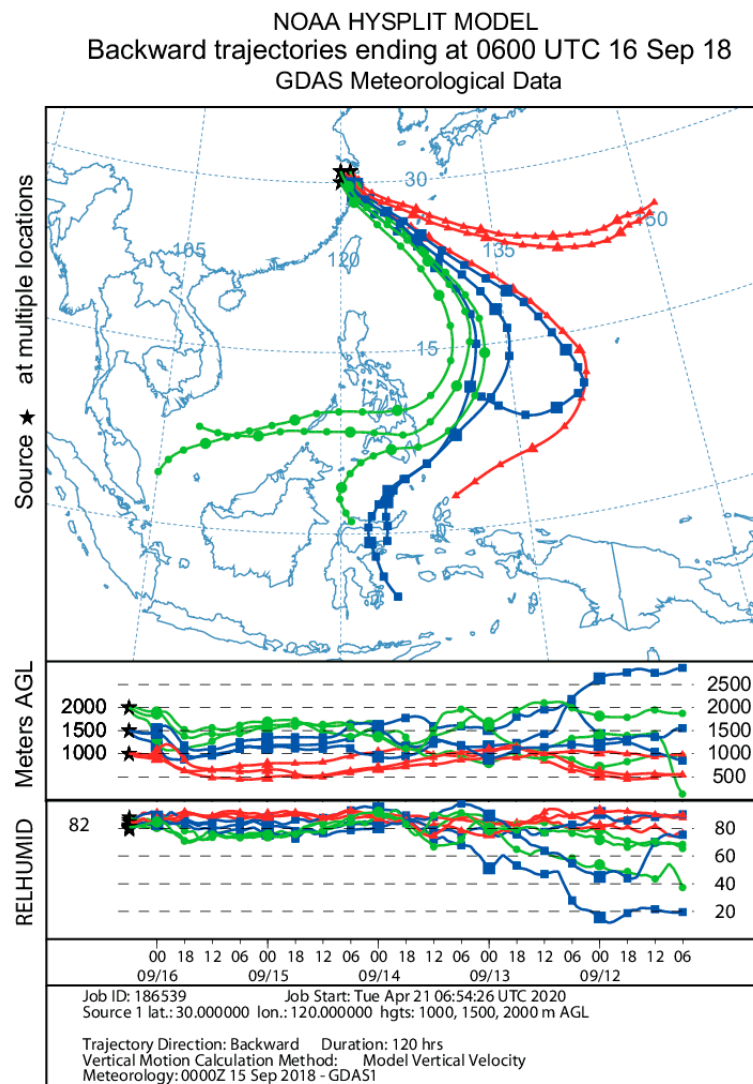


**Figure 10.** The 120-h backward trajectories of above ground level (m) and relative humidity (%) for air parcels located at (120°E, 30°N), (120°E, 31°N), and (121°E, 31°N) at 0600 UTC 16 September 2018 at the above ground level of 1000 m (red lines), 1500 m (blue lines), and 2000 m (green lines).

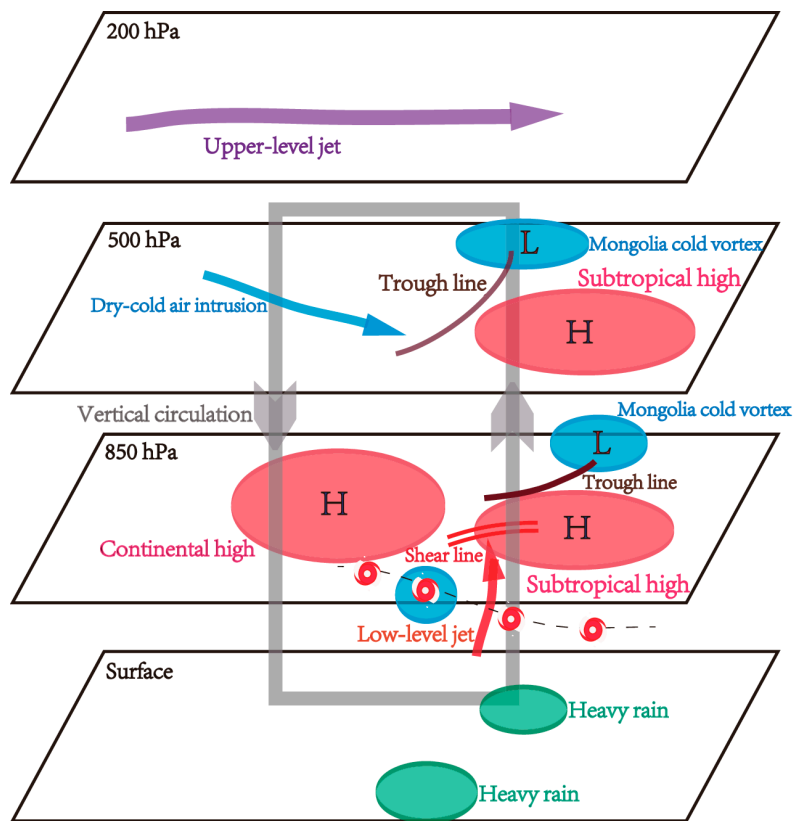


**Figure 11.** Schematic diagram of the physical mechanisms for the remote rainstorm caused by Typhoon Mangkhut.

#### 4. Conclusions

A torrential rain event caused by Typhoon Mangkhut occurred in the Yangtze River Delta on 16 September 2018. A diagnostic analysis was conducted on the causes of the TRR and a trajectory simulation of the moisture source was also performed. As shown in the schematic diagram (Figure 11), the main conclusions are summarized as follows.

- (1) The large-scale circulation situation provides favorable background conditions for the generation of the rainstorm. The rainstorm area is controlled by the subtropical high before the rainstorm, and the high temperature and high humidity are favorable for the accumulation of instability. The cold air behind the trough in Mongolia cold vortex interacts with the low-level warm shear in the rainstorm area. The coupling of the upper and low-level jets increases the low-level convergence and upper level divergence. Moreover, the strengthening of low-level jets and the northward shift of warm shear trigger the release of instability.
- (2) The dry-cold air intrusion in the middle troposphere lasts during the TRR. The intrusion of dry-cold air can increase the convective instability in the precipitation area, and saturate the formerly unsaturated humid air, leading to the rainfall increase.
- (3) The rainstorm area is located at the front edge of the northward-extending high-energy tongue of  $\theta_{se}$ . An obvious convectively unstable stratification appears in the middle and lower troposphere, indicating that the rainstorm is a convective precipitation. The cyclonic vorticity center at the northern end of the typhoon inverted trough appears below 850 hPa. The connection and separation of the cyclonic vortex center and the typhoon center are accompanied by the strengthening and weakening of the precipitation, respectively, indicating that the typhoon provides the dynamic conditions for this rainstorm.

- (4) The main path of moisture transport for this TRR is in the lower troposphere below 850 hPa, connecting the typhoon main body and the TRR area. The moist airmasses in the lower troposphere over the Philippine Sea, the South China Sea, and the sea south of the Philippines are the main sources of moisture for the rainstorm.

At present, there are relatively few studies on TRRs, especially those that occur in the Yangtze River Delta. As numerical weather prediction models often do not resolve TRRs, it is important to understand the influencing factors of TRRs and establish forecast indicators in local areas. The analysis results of the selected case in this paper can provide certain references for rainstorm forecasts in the Yangtze River Delta region when a typhoon approaches South China. The reasons why numerical models failed in predicting this TRR event will be explored in a future study.

**Author Contributions:** Conceptualization, J.Y. and S.G.; methodology, J.Y. and S.G.; formal analysis and investigation, J.Y.; writing—original draft preparation, J.Y.; writing—review and editing, S.G., L.Z., X.S. and L.G. All authors have read and agreed to the published version of the manuscript.

**Funding:** This research was funded by the National Key Research and Development Program of China (Grant No. 2019YFC1510400), the National Natural Science Foundation of China (Grant Nos. 41930967, 41975054), and the Strategic Priority Research Program of the Chinese Academy of Sciences (Grant No. XDA20100304).

**Acknowledgments:** Observational data are provided by the China Meteorological Data Service Center. NCEP GFS analysis and sounding data are provided by the Research Data Archive (RDA) at the U.S. National Center for Atmospheric Research (NCAR). Typhoon best track data are provided by the U.S. Joint Typhoon Warning Center (JTWC). The authors gratefully acknowledge the U.S. NOAA Air Resources Laboratory (ARL) for the provision of the HYSPLIT transport and dispersion model and/or READY website used in this publication. In this paper, we processed datasets and plotted figures using Version 6.6.2 of the NCAR Command Language developed by the NCAR/Computational & Information Systems Laboratory at Boulder, CO, USA, and Version CS6 of Adobe Illustrator manufactured by the Adobe Systems Incorporated at San Jose, CA, USA. We would like to thank Nanjing Hurricane Translation for reviewing the English language quality of this paper.

**Conflicts of Interest:** The authors declare no conflict of interest. The funders had no role in the design of the study; in the collection, analyses, or interpretation of data; in the writing of the manuscript, or in the decision to publish the results.

## References

- Chen, L.; Murata, A.; Duan, Y.; Duong, L.; Ying, L.; Black, P.; Cheng, M. Observations and forecast of rainfall distribution. In Proceedings of the Sixth WMO International Workshop on Tropical Cyclones (IWTC-VI), San Jose, CA, USA, 21–30 November 2006; pp. 36–42.
- Cote, M.R. Predecessor Rain Events in Advance of Tropical Cyclones. Master's Thesis, University at Albany, New York, NY, USA, 2007.
- Cong, C.; Chen, L. An overview on the study of tropical cyclone remote rainfall. *J. Trop. Meteorol.* **2011**, *27*, 264–270. (In Chinese)
- Chen, L. The evolution on research and operational forecasting techniques of tropical cyclones. *J. Appl. Meteorol. Sci.* **2006**, *17*, 672–681. (In Chinese)
- Galarneau, T.J.; Bosart, L.F. Predecessor rain events ahead of tropical cyclones. *Mon. Wea. Rev.* **2010**, *138*, 3272–3297. [[CrossRef](#)]
- Byun, K.-Y.; Lee, T.-Y. Remote effects of tropical cyclones on heavy rainfall over the Korean peninsula—Statistical and composite analysis. *Tellus. A* **2012**, *64*, 14983. [[CrossRef](#)]
- Wang, Y.; Wang, Y. The role of Typhoon Songda (2004) in producing distantly located heavy rainfall in Japan. *Mon. Weather Rev.* **2009**, *137*, 3699–3716. [[CrossRef](#)]
- Zhou, J.; Chen, R.; Li, W. Observational study and prediction of remote rainstorms related to landfalling typhoons. *J. Nanjing Inst. Meteorol.* **1995**, *3*, 376–382. (In Chinese)
- Schumacher, R.S.; Galarneau, T.J. Moisture transport into midlatitudes ahead of recurving tropical cyclones and its relevance in two predecessor rain events. *Mon. Weather Rev.* **2012**, *140*, 1810–1827. [[CrossRef](#)]
- Xu, T.; Li, J.; Yang, Y.; Wang, X.; Chen, B. Verification of SMS-WARMS V2.0 model forecast result. *Meteorol. Mon.* **2016**, *42*, 1176–1183. (In Chinese)
- Ding, Z.; Zhang, X.; He, J.; Xu, H. The study of storm rainfall caused by interaction between the non-zonal high-level jet streak and the far distant typhoon. *J. Trop. Meteorol.* **2001**, *2*, 144–154. (In Chinese)

12. Sun, S.; Zhai, G. On the instability of the low-level jet and its trigger function for the occurrence of heavy rain-storms. *Sci. Atmos. Sin.* **1980**, *4*, 327–337. (In Chinese)
13. Ching, J.; Rotunno, R.; Lemone, M.; Martilli, A.; Kosovic, B.; Jimenez, P.A.; Dudhia, J. Convectively induced secondary circulations in fine-grid mesoscale numerical weather prediction models. *Mon. Wea. Rev.* **2014**, *142*, 3284–3302. [[CrossRef](#)]
14. Chen, J.; Ding, Z. Mesoscale rainstorm system under the coupling of low-level and upper-level jets and typhoon circulation. *Q. J. Appl. Meteorol.* **2000**, *11*, 271–281. (In Chinese)
15. Chen, Q. The instability of the gravity-inertia wave and its relation to low-level jet and heavy rainfall. *J. Meteor. Soc. Japan* **1982**, *60*, 1041–1057. [[CrossRef](#)]
16. Uccellini, L.W.; Johnson, D.R. The coupling of upper and lower tropospheric jet streaks and implications for the development of severe convective storms. *Mon. Weather Rev.* **1979**, *107*, 682–703. [[CrossRef](#)]
17. Li, Y.; Zhao, Y.; Li, T.; Li, M.; Hong, H. Analysis on dry intrusion of a remote typhoon rain. *J. Meteorol. Sci.* **2014**, *34*, 536–542. (In Chinese)
18. Li, C.; Zhao, Y.; Gong, D.; Wang, Y. Numerical simulation of remote typhoon rainstorm in Shandong Province in August 2004. *J. Nanjing Inst. Meteorol.* **2007**, *30*, 503–511. (In Chinese)
19. Draxler, R.R.; Hess, G.D. An overview of the HYSPLIT\_4 modelling system for trajectories dispersion and deposition. *Aust. Meteor. Mag.* **1998**, *47*, 295–308.
20. Stein, A.F.; Draxler, R.R.; Rolph, G.D.; Stunder, B.J.B.; Cohen, M.D.; Ngan, F. NOAA's HYSPLIT atmospheric transport and dispersion modeling system. *Bull. Amer. Meteorol. Soc.* **2015**, *96*, 2059–2077. [[CrossRef](#)]
21. Shan, L.; Tan, G.; Yao, Y.; Wang, Y. On the water vapor condition and moisture transport for a rain caused by a remote tropical cyclone. *J. Trop. Meteorol.* **2014**, *30*, 353–360. (In Chinese)



© 2020 by the authors. Licensee MDPI, Basel, Switzerland. This article is an open access article distributed under the terms and conditions of the Creative Commons Attribution (CC BY) license (<http://creativecommons.org/licenses/by/4.0/>).